Broadband second harmonic generation in one-dimensional randomized nonlinear photonic crystal

Yan Sheng, Dongli Ma, Mingliang Ren, Wenqiang Chai, Zhiyuan Li et al.

Citation: Appl. Phys. Lett. **99**, 031108 (2011); doi: 10.1063/1.3614558
View online: http://dx.doi.org/10.1063/1.3614558
View Table of Contents: http://apl.aip.org/resource/1/APPLAB/v99/i3
Published by the American Institute of Physics.

Broadband second harmonic generation in one-dimensional randomized nonlinear photonic crystal

Yan Sheng,[1,a)] Dongli Ma,[2] Mingliang Ren,[2] Wenqiang Chai,[3] Zhiyuan Li,[2] Kaloian Koynov,[4] and Wieslaw Krolikowski[1]
[1]*Laser Physics Center, Research School of Physics and Engineering, Australian National University, Canberra, ACT 0200, Australia*
[2]*Optical Physics Laboratory, Beijing National Laboratory for Condensed Matter Physics, Institute of Physics, Chinese Academy of Science, Beijing 100080, China*
[3]*Institute of Physikalische Chemie, Johannes Gutenberg-Universitat Mainz, Jakob-Welder-Weg 11, Mainz, 55128, Germany*
[4]*Max-Planck Institute for Polymer Research, Ackermannweg 10, Mainz, 55128, Germany*

(Received 3 June 2011; accepted 30 June 2011; published online 19 July 2011)

We study experimentally second harmonic generation in a one-dimensional nonlinear photonic crystal with randomized inverted-domain structure. We show that the randomness enables one to realize an efficient broadband emission of high-quality second harmonic beam. © *2011 American Institute of Physics*. [doi:10.1063/1.3614558]

Quasi-phase matching (QPM) (Ref. 1) is nowadays the method of choice for efficient frequency conversion of a laser radiation. In the so-called nonlinear photonic crystals (NPCs),[2,3] the QPM conditions can be easily realized by periodic poling of ferroelectric crystals.[4] The resulting spatial modulation of the sign of the nonlinearity $\chi^{(2)}$ enables one to phase match a nonlinear process with wave vector difference that equals the magnitude of some of the reciprocal lattice vectors (RLVs). In order to access broader spectrum of RLVs, so as to get a greater flexibility in phase matching multiple quadratic processes within the same crystal, the QPM has been generalized from a simple one-dimensional (1D) periodic modulation to two-dimensional[5–7] as well as quasi-periodic modulations.[8–10] Moreover, it was shown recently that the use of disordered NPC can relax the stringent phase-matching conditions, thus allowing one to broaden the frequency range that can be converted.[11] The observation of such broadband second harmonic (SH) has been reported in naturally grown strontium barium niobate (SBN) crystal that has random-size ferroelectric domains in 2D plane.[12,13] However, the interactions in such totally randomized crystals suffer from extremely low conversion efficiency. This problem has been solved by employing a 2D short-range ordered NPC, which can convert the frequency of a broadband source with efficiency of $\sim 12\%$.[14] The concept of such short-range ordered structure has been recently proposed to enhance the transmission of broadband terahertz wave[15] and to extend the wavelength acceptance bandwidth of a nonlinear process (from typical 2-4 nm to 20 nm).[16]

While valuable progress has been achieved, the broadband frequency conversions that have been investigated in NPC so far suffer from the high divergence of the generated harmonic beams. When a Gaussian beam is used to illuminate the naturally random crystals or the engineered short-range ordered NPC, the emitted SH wave always form a line in far field.[12–14] The measured divergence angle is typically no less than 5° in the horizontal direction, which limits the practical use of such broadband SHG. In this letter, we solve this problem by proposing an advanced distribution of ferroelectric domains in 1D randomized structure. Consequently, we demonstrate an efficient broadband SHG which perfectly represents the spatial intensity profile of the fundamental beam.

In experiment, we fabricated the 1D randomized NPC via standard electric-field poling of a Z-cut $LiNbO_3$ wafer. The length, width, and thickness of the poled sample were, respectively, 9.6, 9.6, and 0.4 mm. The inverted-domain structure visualized by surface etching is shown in Fig. 1(a). This random domain distribution was created as follows. First, we chose a line segment (length $2a$). Then, we built a 1D periodic lattice (lattice constant b) and located the line segment centered at each lattice point. After this, we randomly rotated each line segment around its own center. Finally, we placed the rectangular domain-inverted region vertically at each endpoint of these line segments [see the

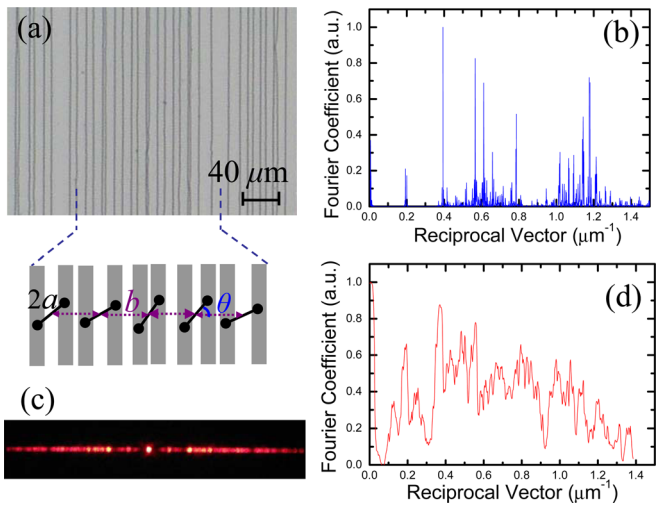

FIG. 1. (Color online) (a) The 1D randomized domain pattern imaged by acid etching. The expanded view show how the randomness is created. (b) Theoretical spectrum of reciprocal vectors obtained by Fourier transform. (c) Diffraction pattern of the sample by He-Ne laser. (d) Experimental spectrum of the reciprocal vectors.

a)Electronic mail: ysh111@physics.anu.edu.au.

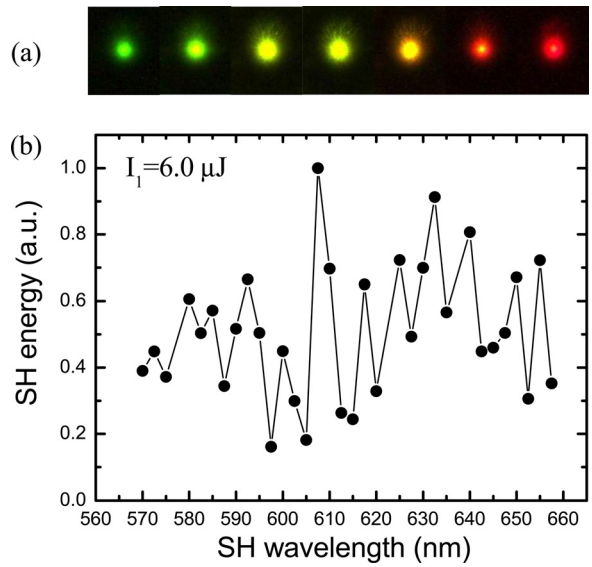

FIG. 2. (Color online) (a) The images of the spatial profiles of the emitted SH beams. From left to right, the SH wavelength is $\lambda_2 = 570.0$, 575.0, 580.0, 585.0, 587.5, 610.0, and 640.0 nm, respectively. (b) The wavelength tuning curve of SHG obtained with the same pump pulse energy.

expanded view of Fig. 1(a)]. The resulting domain (and consequently, nonlinearity) pattern can be expressed as

$$g(x) = rect(x/l) \otimes \sum_{m=-M}^{M} [\delta(x - mb - a\cos\theta_m + a\sin\theta_m) + \delta(x - mb + a\cos\theta_m - a\sin\theta_m)]. \quad (1)$$

Here, the rectangle function *rect* is defined by $rect(x/l) = 1$ when $|x| < l/2$ and $rect(x/l) = 0$ elsewhere; $\otimes$ is the convolution operator; m is an integer; θ_m represents the rotation angle of the mth line segment and M defines the number of the total line segments.

Upon taking the Fourier transform of the structure function $g(x)$, we obtain the spectrum of reciprocal lattice vectors that can be used for quasi-phase matching of frequency conversion processes. Assuming negligible pump depletion and weak focusing, the interaction efficiency is proportional to the square of the relevant Fourier coefficient, which can be written as

$$|G(k_x)|^2 = A \sum_{m,m'=-M}^{M} B_m B_{m'} \cos[2\pi b(m - m')k_x]. \quad (2)$$

Here, $A = 4l\mathrm{sinc}(lk_x)/b$ with $\mathrm{sinc}(x) = \sin(x)/x$ and $B_m = \cos[\pi a k_x(\cos\theta_m - \sin\theta_m)]$. In Fig. 1(b), we plot the $|G(k_x)|^2$ using the structure parameters of the real sample: $a = 12$ μm, $b = 32$ μm, $l = 2$ μm, and θ takes random value from $[0, \pi/4]$. As can be seen, the reciprocal vectors of this 1D randomized structures exhibit continuous distribution in some regions of the wave vector k_x, which are ideal for broadband frequency conversions. The Fourier coefficients in these continuous regions are larger than those associated with a completely randomized structure, making the nonlinear interactions much more efficient. In Figs. 1(c) and 1(d), we show experimentally observed diffraction pattern of the randomized NPC oriented with its optical axis parallel to the incident He-Ne laser beam. The results agree quite well with calculations. The experimental spectrum of the reciprocal vectors is slightly broader than that of the theoretically predicted, which can be attributed to the fabrication imperfection of the domain-inverted structures.

For the broadband frequency conversion experiment, we use a light beam from optical parametric generator-amplifier generating 16 ps pulses with a repetition rate of 10 Hz. The laser beam is *s*-polarized and propagates along the *x* crystallographic axis of the sample in order to take advantage of the largest nonlinear coefficient d_{33} of $LiNbO_3$ crystal. The beam is loosely focused so that the beam waist at the input facet of the sample is about 50 μm. This beam size corresponds to intensities of up to 9 GW/cm^2 for the range of input powers used in the experiments. The generated SH emission is either directed to a power meter or projected on a screen located 10 mm behind the crystal and then imaged by a CCD camera.

In experiment when the laser wavelength is continuously tuned from 1130 nm to 1320 nm, the corresponding SH is observed all the time with its color changing continuously from green to red. In Fig. 2(a), we display the recorded images of such SH waves for varying wavelength of the fundamental beam. Moreover, it can be seen from this figure that the SH waves are observed as bright spots, which indicates the spatial profile of the fundamental wave is preserved very well. In Fig. 2(b), we depict the wavelength tuning curves of the SHG, i.e., the energy of the emitted SH vs. fundamental wavelength, with constant input pulse energy of 6.0 μJ. It is seen that while the harmonic energy varies with the wavelength, the efficient frequency doubling process is observed at all wavelengths. The fluctuation of these SH pulse energies reflects the variation of the square of the Fourier coefficients of the corresponding RLVs. It is worth noting that the operational

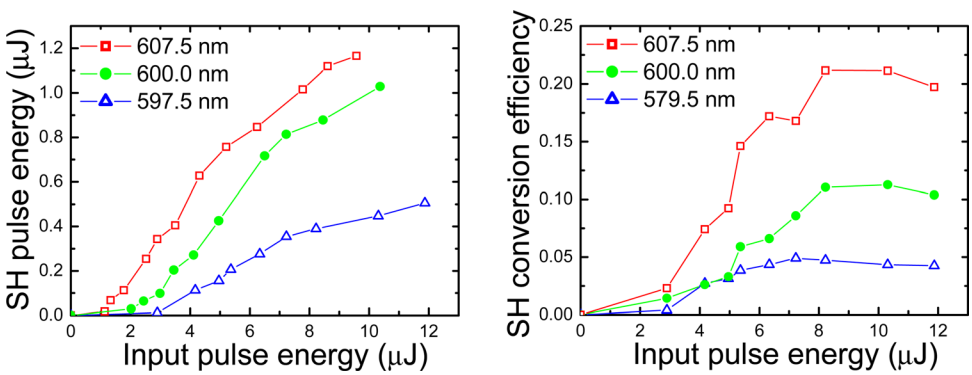

FIG. 3. (Color online) (a) SH pulse energies and (b) conversion efficiencies vs. pulse energy of the input fundamental beam.

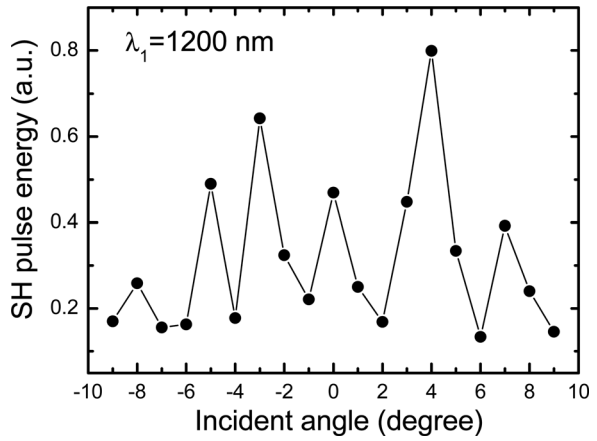

FIG. 4. Experimentally recorded SH pulse energy as a function of the incidence angle of the fundamental beam.

frequency range of our randomized structure could have been even wider than the presented here. For the SHG from 1130 nm to 1320 nm, we used the RLVs from 0.49 to 0.74 μm^{-1}. However, as shown in Figs. 1(b) and 1(d), there are still longer RLVs $k_x \in [0.98, 1.31]\mu m^{-1}$. These RLVs in principle can lead to the SHG from 955 nm to 1045 nm. We did not put this frequency range into experimental study because of the limitation of our pump laser source.

In Figs. 3(a) and 3(b), we show the measured pulse energy and conversion efficiency for the SHG in the randomized structure. Here, we only depict results for the SHG emitted at $\lambda_2 = 607.5$, 600.0, and 597.5 nm, which are representative for the harmonic generations with higher, middle, and lower conversion efficiencies in the whole investigated frequency range. It is seen that the SH conversion efficiency increases gradually with input energy at a low excitation limit (when the input energy is less than 8.0 μJ). Then, it reaches saturation when the input energy goes higher, which can be attributed to the back conversion effect ($\omega_2 - \omega_1 = \omega_1$). The saturation of the conversion efficiency is 21%, 11%, and 5% for the SHG at 607.5, 600.0, and 597.5nm, respectively.

In Fig. 4, we display the experimentally recorded SH signal as a function of the incident angles of the fundamental beam (taking the result of SHG at $\lambda_2 = 600$ nm as a representative of the whole investigated frequency range). It is very interesting to see that unlike the case of fully periodic domain structures which is very sensitive to the angular tuning with the SH signals dropping to zero very quickly, the randomized structures enables one to obtain strong frequency conversion for a relatively large incidence angle. This property is a direct consequence of the almost continuous distribution of reciprocal vectors available in the randomized structure. With the tuning of the incident angle, the corresponding reciprocal vector required for the efficient SHG varies as $G = 2\pi(\sqrt{n_2^2 - n_1^2 \sin^2\theta} - n_1\cos\theta)/\lambda_2$. For periodic structures, there are only discrete reciprocal vectors. So the SH signal drops dramatically when the angle θ is tuned away from the predesigned value. However, for the randomized structures, the continuous distribution of reciprocal vectors, i.e., the infinite set of G, allows the fulfillment of the phase-matching conditions for each incident angle. Being similar to the case of wavelength tuning, the angle tuning curve of the SHG also reflects the strength of the corresponding reciprocal vectors.

In conclusion, we have designed and fabricated a nonlinear photonic crystal in $LiNbO_3$ sample with 1D randomized domain reversal structure and have realized broadband SH emission in the green and red regions of the spectrum with conversion efficiency varying from 5% to 20%. Moreover, we have shown that the interaction results in the high quality of the transverse profile of the second harmonic beam for all emission frequencies. We believe that the approach presented here can be also used for the broadband third and fourth harmonic generation in a single crystal.

We thank C. Bubeck for the helpful discussions. The authors acknowledge financial support from the Australian Research Council and Australian Academy of Science.

[1]J. A. Amstrong, N. Bloembergen, J. Ducuing, and P. S. Pershan, Phys. Rev. **127**, 1918 (1962).
[2]V. Berger, Phys. Rev. Lett. **81**, 4136 (1998).
[3]A. Arie and N. Voloch, Laser Photon. Rev. **4**, 355 (2010).
[4]M. Houe and P. D. Townsend, J. Phys. D **28**, 1747 (1995).
[5]N. G. R. Broderick, G. W. Ross, H. L. Offerhaus, D. J. Richardson, and D. C. Hanna, Phys. Rev. Lett. **84**, 4345 (2000).
[6]L. H. Peng, C. C. Hsu, and Y. C. Shih, Appl. Phys. Lett. **83**, 3447 (2003).
[7]P. Xu, S. H. Ji, S. N. Zhu, X. Q. Yu, J. Sun, H. T. Wang, J. L. He, Y. Y. Zhu, and N. B. Ming, Phys. Rev. Lett. **93**, 133904 (2004).
[8]S. Zhu, Y. Zhu, and N. Ming, Science **278**, 843 (1997).
[9]R. T. Bratfalean, A. C. Peacock, N. G. R. Broderick, and K. Gallo, Opt. Lett. **30**, 424 (2005).
[10]Y. Sheng, J. Dou, B. Cheng, and D. Zhang, Appl. Phys. B: Lasers Opt. **87**, 603 (2007).
[11]S. E. Skipetrov, Nature (London) **432**, 285 (2004).
[12]R. Fisher, S. M. Saltiel, D. N. Neshev, W. Krolikowski, and Yu. S. Kivshar, Appl. Phys. Lett. **89**, 191105 (2006).
[13]W. Wang, K. Kalinowski, V. Roppo, Y. Sheng, K. Koynov, Y. Kong, C. Cojocaru, J. Trull, R. Vilaseca, and W. Krolikowski, J. Phys. B: At. Mol. Opt. Phys. **43**, 215404 (2010).
[14]Y. Sheng, J. Dou, B.Ma, B. Cheng, and D. Zhang, Appl. Phys. Lett. **91**, 011101 (2007).
[15]A. Agrawal, T. Matsui, Z. V. Vardeny, and A. Nahata, Opt. Express **16**, 6267 (2008).
[16]I. Varon, G. Porat, and A. Arie, *paper presented at the Thirteenth Meeting on Optical Engineering and Science in Israel*, Tel-Aviv, Israel, 9–10 March 2011.